

1 **The Value of Normal Interictal EEGs in Epilepsy Diagnosis and Treatment Planning: A Retrospective**  
2 **Cohort Study using Population-level Spectral Power and Connectivity Patterns**

3 Neeraj Wagh<sup>1</sup>, Andrea Duque-Lopez<sup>2</sup>, Boney Joseph<sup>2</sup>, Brent Berry<sup>2</sup>, Lara Jehi<sup>3</sup>, Leland Barnard<sup>2</sup>,  
4 Venkatsampath Gogineni<sup>2</sup>, Benjamin H. Brinkmann<sup>2</sup>, David T. Jones<sup>2</sup>, Gregory Worrell<sup>2,\*</sup>, Yogatheesan  
5 Varatharajah<sup>1,4,\*</sup>

6 <sup>1</sup> Department of Bioengineering, University of Illinois, Urbana, IL 61801

7 <sup>2</sup> Department of Neurology, Mayo Clinic, Rochester, MN 55905

8 <sup>3</sup> Department of Neurology, Cleveland Clinic, Cleveland, OH 44195

9 <sup>4</sup> Department of Computer Science, University of Minnesota, Minneapolis, MN 55455

10 (\*co-corresponding authors)

11  
12  
13  
14  
15  
16  
17  
18  
19  
20  
21  
22  
23  
24  
25  
26  
27  
28  
29  
30  
31  
32  
33  
34  
35  
36  
37  
38  
39  
40  
41  
42

## 1 **Abstract**

2 *Introduction:* Scalp electroencephalography (EEG) is a cornerstone in the diagnosis and treatment of  
3 epilepsy, but routine EEG is often interpreted as normal without identification of epileptiform activity  
4 during expert visual review. The absence of interictal epileptiform activity on routine scalp EEGs can  
5 cause delays in receiving clinical treatment. These delays can be particularly problematic in the diagnosis  
6 and treatment of people with drug-resistant epilepsy (DRE) and those without structural abnormalities  
7 on MRI (i.e., MRI negative). Thus, there is a clinical need for alternative quantitative approaches that can  
8 inform diagnostic and treatment decisions when visual EEG review is inconclusive. In this study, we  
9 leverage a large population-level routine EEG database of people with and without focal epilepsy to  
10 investigate whether normal interictal EEG segments contain subtle deviations that could support the  
11 diagnosis of focal epilepsy.

12 *Data & Methods:* We identified multiple epochs representing eyes-closed wakefulness from 19-channel  
13 routine EEGs of a large and diverse neurological patient population (N=13,652 recordings, 12,134 unique  
14 patients). We then extracted the average spectral power and phase-lag-index-based connectivity within  
15 1-45Hz of each EEG recording using these identified epochs. We decomposed the power spectral density  
16 and phase-based connectivity information of all the visually reviewed normal EEGs (N=6,242) using  
17 unsupervised tensor decompositions to extract dominant patterns of spectral power and scalp  
18 connectivity. We also identified an independent set of routine EEGs of a cohort of focal epilepsy patients  
19 (N= 121) with various diagnostic classifications, including focal epilepsy origin (temporal, frontal), MRI  
20 (lesional, non-lesional), and response to anti-seizure medications (responsive vs. drug-resistant epilepsy).  
21 We analyzed visually normal interictal epochs from the EEGs using the power-spectral and phase-based  
22 connectivity patterns identified above and evaluated their potential in clinically relevant binary  
23 classifications.

24 *Results:* We obtained six patterns with distinct interpretable spatio-spectral signatures corresponding to  
25 putative aperiodic, oscillatory, and artifactual activity recorded on the EEG. The loadings for these  
26 patterns showed associations with patient age and expert-assigned grades of EEG abnormality. Further  
27 analysis using a physiologically relevant subset of these loadings differentiated focal epilepsy patients  
28 from controls without history of focal epilepsy (mean AUC 0.78) but were unable to differentiate  
29 between frontal or temporal lobe epilepsy. In temporal lobe epilepsy, loadings of the power spectral  
30 patterns best differentiated drug-resistant epilepsy from drug-responsive epilepsy (mean AUC 0.73), as  
31 well as lesional epilepsy from non-lesional epilepsy (mean AUC 0.67), albeit with high variability across  
32 patients.

33 *Significance:* Our findings from a large population sample of EEGs suggest that normal interictal EEGs of  
34 epilepsy patients contain subtle differences of predictive value that may improve the overall diagnostic  
35 yield of routine and prolonged EEGs. The presented approach for analyzing normal EEGs has the capacity  
36 to differentiate several diagnostic classifications of epilepsy, and can quantitatively characterize EEG  
37 activity in a scalable, expert-interpretable, and patient-specific fashion. Further technical development  
38 and clinical validation may yield normal EEG-derived computational biomarkers that could augment  
39 epilepsy diagnosis and assist clinical decision-making in the future.

40 **Keywords:** normal interictal EEGs, quantitative EEG analysis, spectral power, phase lag index, focal  
41 epilepsy, non-lesional epilepsy, drug-resistant epilepsy, unsupervised learning, tensor decomposition

## 1 1. Introduction

2 Epilepsy is a neurological disorder characterized by recurrent, unprovoked seizures and is estimated to  
3 affect ~50 million people worldwide<sup>1</sup>. A scalp electroencephalogram (EEG) non-invasively records the  
4 electrical activity of the brain, and its findings play a critical role in the clinical diagnosis and  
5 management of epilepsy<sup>2-4</sup>. The diagnostic yield of a short 20–40-minute routine EEG is determined by  
6 the presence of spontaneous transient interictal epileptiform discharges (IEDs)<sup>5-7</sup>. However, ~30-55% of  
7 routine EEGs of patients with epilepsy and 9-10% of prolonged video EEGs show no evidence of IEDs and  
8 delay the diagnosis of epilepsy<sup>12-17</sup>.

9 In newly diagnosed epilepsy, anti-seizure medications (ASMs) are the first choice of therapy. However,  
10 despite a successful diagnosis, about half the patients do not respond to their first ASM, and about a  
11 third continue to have uncontrolled seizures despite multiple ASM trials<sup>14,15</sup>. Therefore, the  
12 determination of drug-resistant epilepsy (DRE) can take several months or years, while the patients  
13 continue to experience seizures and comorbidities. Thus, the early identification of DRE is essential to  
14 reduce disease burden and to initiate evaluations for additional therapies such as resective surgery and  
15 electrical brain stimulation. In focal epilepsy, magnetic resonance imaging (MRI) scans of the brain can  
16 help clarify the disease etiology by identifying structural abnormalities that lead to seizures<sup>16</sup>. In MRI  
17 negative, i.e., non-lesional, epilepsy patients, normal EEGs can cause further delays in identifying the  
18 epileptogenic brain regions for treatment. Broadly, the inability to identify interictal epileptiform activity  
19 during visual review of routine EEGs can delay the initiation of ASMs, increase healthcare costs<sup>18</sup>, and put  
20 the patient at an increased risk of seizure-related injuries and comorbidities<sup>18,19</sup>.

21 As such, there is a clear need for alternative approaches that can assist with early diagnosis and  
22 treatment planning when traditional routine EEG tests are inconclusive. Our goal in this study is to  
23 develop a quantitative approach to explore automatic analysis normal interictal EEGs, which could  
24 provide early, objective, and inexpensive clinical decision support. Emerging evidence suggests that such  
25 quantitative approaches have the potential to improve the diagnostic value of normal EEGs and augment  
26 decision-making in epilepsy<sup>17-20</sup>. Building on prior work, here we take a data-driven approach --  
27 leveraging a large population database -- to identify spectral power and connectivity patterns of normal  
28 interictal EEG and evaluate their potential in differentiating various focal epilepsy classifications.

29 In this study, we retrospectively analyzed a large dataset of 13,652 routine EEGs from a diverse  
30 neurological population of 12,134 adults and a cohort of 121 adults with confirmed focal epilepsy.  
31 Patterns of power spectral density and phase-based connectivity in eyes-closed wakefulness were  
32 extracted from the 6,242 normal EEGs in the population dataset using canonical polyadic tensor  
33 decomposition. We examined the spatial and frequency distributions of these patterns and investigated  
34 their association with age and clinically assigned EEG grades. Then, pattern loadings were computed to  
35 quantitatively characterize the normal EEG activity (i.e., interictal non-epileptiform) of patients with focal  
36 epilepsy. With these loadings, we studied group differences and conducted classification analyses to  
37 explore the use of normal EEGs in epilepsy diagnosis and treatment planning.

38 We found that data-driven decomposition of spectral power and connectivity of normal EEGs yields  
39 patterns that are interpretable in terms of known scalp electrophysiology and sensitive to physiological  
40 and pathological changes. Furthermore, the quantification of expert visual review normal interictal EEG  
41 activity using these patterns revealed relevant group differences in focal epilepsy. These results suggest  
42 that quantitative characterization of normal interictal EEGs of focal epilepsy patients has the potential to

1 augment visual EEG review and assist clinical decision-making in epilepsy. Future efforts will focus on  
2 validating these findings using a larger out-of-sample epilepsy cohort with data collected from an  
3 external site.

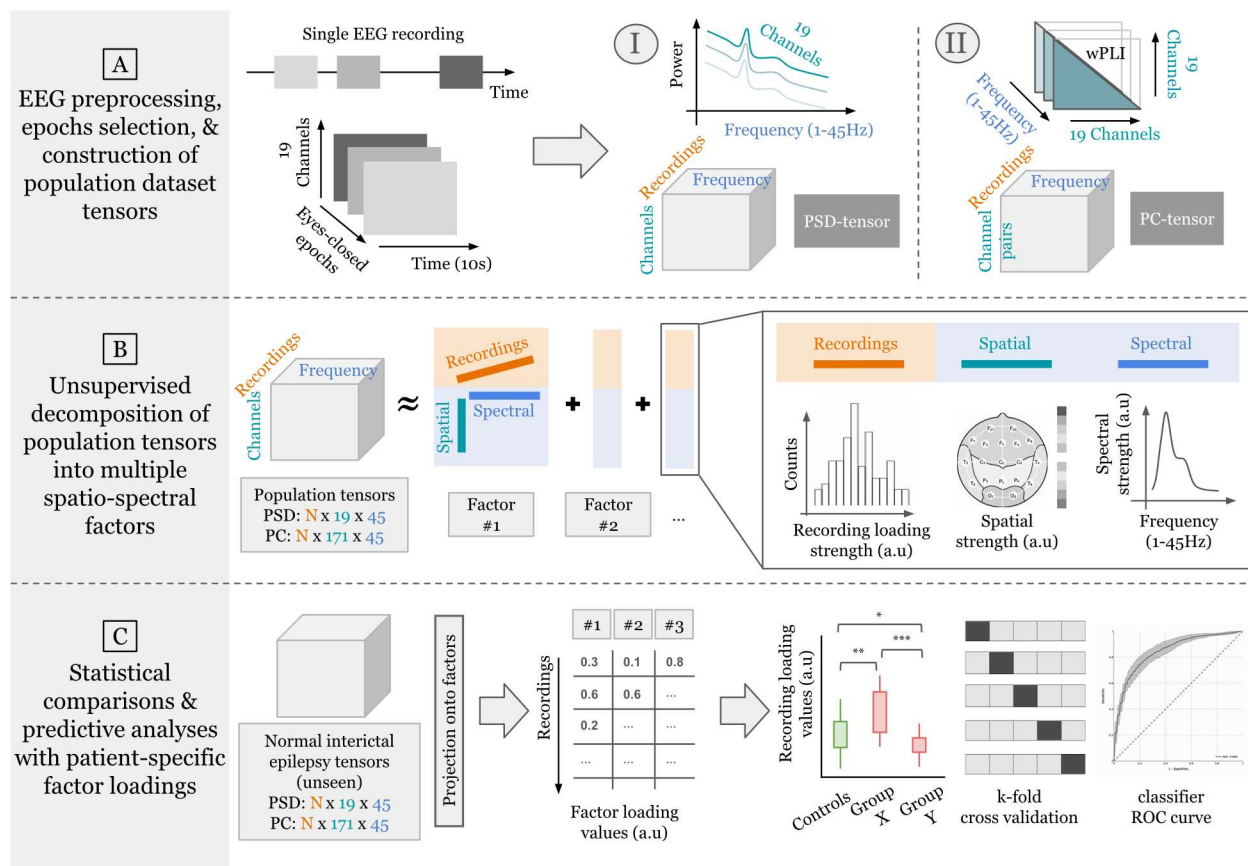
4

## 5 **2. Data & Methods**

6 **Clinical population dataset and expert EEG review:** Our study utilized 13,652 routine clinical EEG  
7 recordings obtained from 12,134 adult patients (18 or older) at Mayo Clinic, Rochester, MN, USA  
8 between 2016 and 2022<sup>21</sup>. This study was approved by the Mayo Clinic institutional review board and  
9 patients provided informed consent. The EEGs were recorded using the XLTEK EMU40EX headbox  
10 manufactured by Natus Medical Incorporated, Oakville, Ontario, Canada. All EEGs followed the standard  
11 10–20 electrode placement system<sup>22</sup> and were sampled at 256Hz. The patient population comprises  
12 individuals presenting with a diverse array of conditions including epilepsy, cognitive impairment,  
13 episodic migraines, syncope, and functional spells, among others. Overall, this dataset represents the  
14 patient population typically referred for routine EEG assessments at the Mayo Clinic in Rochester, MN,  
15 USA. All EEG records were visually reviewed by board-certified epileptologists and graded based on the  
16 Mayo Clinic internal EEG grading protocol: Normal (no visible abnormalities, within normal limits),  
17 asymmetry, persistent delta frequency slowing, and intermittent abnormalities classified as Dysrhythmia  
18 1 (mild, non-specific slowing or excess of fast activity), Dysrhythmia 2 (moderate to severe intermittent  
19 slowing), or Dysrhythmia 3 (e.g. epileptiform abnormalities, triphasic waves, intermittent rhythmic delta  
20 frequency activity).

21 **Focal epilepsy cohort and matched control subjects without epilepsy:** Patients with EEGs containing  
22 focal epileptiform abnormalities were used to triage focal epilepsy cases in the overall patient  
23 population. Based on further review of those patients, we identified a total of 121 focal epilepsy patients  
24 (frontal=21; temporal=100) who had a confirmed diagnosis of frontal or temporal lobe epilepsy and had  
25 no prior history of any cranial surgery. Their drug response status and MRI findings were determined by  
26 reviewing electronic health records and diagnostic MRI reports available within a year of their EEG  
27 assessments, respectively. An age- and sex-matched control cohort of 76 subjects without epilepsy  
28 diagnosis with normal EEGs was selected for comparisons. Data of patients in focal epilepsy and matched  
29 control sets were excluded from the population set during subsequent analyses to prevent statistical  
30 data leakage.

31



1  
2 *Figure 1: Overall analytic workflow of the study. (A) Multiple eyes-closed awake interictal epochs from*  
3 *each EEG recording are identified for data analysis. The average power spectral density (PSD) and phase-*  
4 *based connectivity (PC) between each channel pair are computed and stacked across recordings to obtain*  
5 *3-d PSD and PC tensors (recordings x channels or channel pairs x frequencies). (B) PSD and PC population*  
6 *tensors are decomposed separately in an unsupervised fashion to obtain multiple interpretable spatio-*  
7 *spectral patterns (i.e., factors). (C) Normal interictal EEG data from focal epilepsy patients are projected*  
8 *on each population-level factor to obtain patient-specific factor loadings. Differences in drug-resistant*  
9 *and non-lesional MRI focal epilepsy are investigated by using these loadings in statistical group/sub-*  
10 *group comparisons and predictive analyses.*

11 The complete analytical workflow of this study from processing of raw EEGs to results is illustrated in  
12 Figure 1. Below we describe the methods used in this workflow.

13 **EEG preprocessing and epochs selection:** All routine EEGs were preprocessed as follows: 1) selection  
14 and ordering of the 19 EEG channels arranged according to the 10-20 system (i.e., Fp1, F3, F7, C3, T7, P3,  
15 P7, O1, Fp2, F4, F8, C4, T8, P4, P8, O2, Fz, Cz, and Pz), 2) resampling to ensure a sampling rate of 256 Hz,  
16 3) band-pass filtering between 0.1-45Hz, and 4) transformation to common average reference. We note  
17 that no explicit artifact rejection step was performed in this pipeline. Next, we applied a heuristic  
18 algorithm<sup>23</sup> to select a maximum of six 10-second EEG epochs from the full recording representing eyes-  
19 closed wakefulness. The algorithm relies on sleep staging<sup>24</sup>, eye blinks, sample entropy, and occipital  
20 alpha power to select candidate epochs. These selected epochs are not guaranteed to be contiguous.  
21 After preprocessing, all EEG recordings were represented by at most six EEG epochs representing eyes-

1 closed resting-state wakefulness. Preprocessing was done using the numpy<sup>25</sup> and MNE<sup>26</sup> Python libraries.  
2 Epochs selection used the MNE-features<sup>27</sup> and YASA<sup>28</sup> libraries.

3 **Manual review of EEG epochs extracted from focal epilepsy patients:** A board-certified epileptologist  
4 visually identified interictal segments automatically derived from the EEGs of focal epilepsy patients,  
5 excluding abnormal segments containing seizures, epileptiform spikes, epileptiform sharp waves,  
6 temporal intermittent rhythmic delta activity (TIRDA), and excessive artifacts. Polymorphic, intermittent  
7 delta and theta frequency slowing (0.1 - <8 Hz) events, however, could not be excluded due to their  
8 pervasive presence in some EEGs.

9 **Constructing tensors of spectral power:** Power spectral density (PSD) of EEG data was estimated for all  
10 19 EEG channels using Welch's algorithm<sup>29</sup>, yielding log-power values at all integer frequencies between  
11 1-45Hz. We then averaged the PSD measures of each EEG recording across all the identified epochs to  
12 obtain a single PSD vector for each channel. The PSD measures of each EEG recording can now be  
13 represented as a matrix with shape 19 × 45 (19 channels and 45 frequencies). Stacking this average PSD  
14 matrix across recordings produces a 3-d power-spectral tensor ("PSD-tensor") of the form: N recordings  
15 x 19 channels x 45 frequencies. The population PSD-tensor is globally min-max scaled between [0, 1] to  
16 maintain non-negativity for subsequent tensor decomposition. Focal epilepsy and control PSD-tensors  
17 are scaled similarly but are stacked together first to preserve group differences for downstream analyses.

18 **Constructing tensors of phase-based connectivity:** An estimate of phase-based connectivity (PC)  
19 between a pair of channels ( $i, j$ ) is computed using the weighted Phase Lag Index<sup>30</sup> (wPLI) measure  
20 defined as:

21 
$$wPLI(i, j) = \frac{|E[\mathcal{J}(X_{ij})]|}{E[|\mathcal{J}(X_{ij})|]}$$

22 where  $X_{i,j}$  denotes the cross-spectral density of channels  $i$  and  $j$ ,  $\mathcal{J}(\cdot)$  is the imaginary part of the cross-  
23 spectrum, and  $E[\cdot]$  represents a mean over the selected eyes-closed epochs. wPLI values range between  
24 [0, 1]. A positive value reflects an imbalance between leading and lagging relationships, with 1 indicating  
25 a perfect lead or lag relationship. At each integer frequency between 1-45Hz, wPLI provides a  
26 connectivity value for each of the 171 unique channel pairs. Thus, we obtain a 3-d phase-based  
27 connectivity tensor ("PC-tensor") of the form: N recordings x 171 channel pairs x 45 frequencies.

28 **Representing the normal EEGs as tensors:** We estimated the PSD and PC measures for the normal EEGs  
29 in the population dataset (N=6,242) and formed the population PSD-tensor and PC-tensor of shape  
30 (6,242 x 19 x 45) and (6,242 x 171 x 45), respectively.

31 **Decomposition of 3-d tensors into factors:** The canonical polyadic (CP) decomposition<sup>31,32</sup> (also known  
32 as the PARAFAC decomposition<sup>33</sup>) approximates a given tensor as a sum of  $R$  rank-1 tensors, where  $R$   
33 is the decomposition rank, i.e., the resulting number of factors obtained from decomposing the tensor. The  
34 CP decomposition of a 3-dimensional tensor  $T$  with rank  $R$  is defined as:

35 
$$T \approx \sum_{r=1}^R A_r \otimes B_r \otimes C_r$$

1 where  $\otimes$  denotes an outer product and  $A_r$ ,  $B_r$ , and  $C_r$  are vectors with shapes matching each of the  
2 three dimensions of  $T$  (recording, channel, frequency). Each term in the summation, i.e., a combination  
3 of  $A_r$ ,  $B_r$ , and  $C_r$ , is a rank-1 tensor and is referred to as a factor. The  $A$ ,  $B$ , and  $C$  factor matrices  
4 (containing  $A_r$ ,  $B_r$ , and  $C_r$  vectors as columns, respectively) are optimized with a non-negativity  
5 constraint using the hierarchical alternating least squares<sup>33,34</sup> approach.

6 **Determining the initialization and rank for CP decomposition:** We provided a physiologically meaningful  
7 initialization and rank derived from PSD characteristics of healthy subjects to initialize the decomposition  
8 of the PSD-tensor. For this, we fit a parametric model of the EEG PSD, named FOOOF<sup>35</sup> (“fitting  
9 oscillations and one over  $f$ ”), to the eyes-closed trials in the MPI Leipzig Mind-Brain-Body dataset<sup>36</sup>  
10 (N=207, 8 trials per subject, 60s trial duration). The FOOOF model segments the observed morphology of  
11 an EEG PSD into superimposed aperiodic ( $L$ ) and oscillatory components ( $G_n$ ):

$$12 \quad PSD = L + \sum_{n=1}^5 G_n$$

13 Each  $G_n$  is a Gaussian peak corresponds putatively to a canonical brain oscillation (delta, theta, alpha,  
14 beta, or gamma) and is parameterized by height, mean or center frequency, and a standard deviation.  $L$   
15 is a function of the form  $L(F) = 10^b * \frac{1}{(k+F^\chi)}$  whose parameters  $b$ ,  $k$ , and  $\chi$  capture aperiodic 1/f-like  
16 nature of the  $PSD$ . We refer readers to Donoghue et. al. (2020) for additional model details. We fit this  
17 six-component model to healthy PSDs in the MPI-Leipzig dataset. The fitted versions of  $G_n$  and  $L$  formed  
18 the frequency initializations  $B_r$  of the decomposition solution and informed the choice of rank  $R = 6$ .

19 **Decomposing the population tensors:** Factor matrix  $B$  (containing  $B_r$  vectors as columns) was initialized  
20 with the six spectral “priors” described above. CP decomposition with non-negativity constraints and  
21  $R=6$  was applied on the min-max scaled population PSD-tensor. The resultant  $B$  was then used as an  
22 immutable initialization for the subsequent CP decomposition of the population PC-tensor. In other  
23 words, only factor matrices  $A$  and  $C$  were optimized in the PC-tensor decomposition. The use of  $B$ , i.e.,  
24 frequency patterns extracted from the PSD-tensor, in PC factors ensured that interpretations were  
25 aligned across both decompositions. Tensor analyses were done using the `tensortools`<sup>36</sup> Python library.

26 **Visualization of factors derived from the normal EEG population:** The  $A_r$ ,  $B_r$ , and  $C_r$  vectors resulting  
27 from both CP decompositions represent semantically coherent components:  $A_r$  contains factor’s  
28 loadings per recording,  $B_r$  holds the factor’s channel activations, and  $C_r$  holds the factor’s frequency  
29 activations. The recording loadings are visualized as histograms, channel activations as topographical  
30 distributions over the scalp, and frequency activations as power spectral profiles. Note that we obtain  $A_r$   
31 and  $C_r$  separately from the PSD-tensor and PC-tensor decompositions, while  $B_r$  is shared between both  
32 as described above. We refer to values in  $A_r$  as “PSD loadings” or “PC loadings” depending on the tensor  
33 they are associated with.

34 **Computing factor loadings for the focal epilepsy cohort:** We computed population factor loadings for  
35 the focal epilepsy cohort using a projection operation<sup>37</sup>. Consider the basis matrix  $P$  containing  
36 vectorized versions of the spatio-spectral factors  $B_r \otimes C_r$ . Thus, matrix  $P$  has  $R$  rows and  $C * F$  columns,  
37 where  $C$  and  $F$  is the length of the channel dimension and frequency dimension of the tensor,  
38 respectively. Then, for a new EEG recording  $x_{new} \in R^{C * F}$ , its loadings are computed by  
39  $P^+ \times \text{vectorized}(x_{new})$ , where  $P^+$  is the pseudo-inverse of  $P$ . The results of this operation are weights

1 or loadings representing how strongly each factor is expressed in the new recording. Note that this  
2 operation does not guarantee non-negative loadings.

3 **Associations and statistical testing:** Pearson’s correlation coefficient and Spearman’s rank correlation  
4 coefficient were used to quantify associations of factor loadings with patient age and ranked degree of  
5 slowing, respectively. The corresponding p-values test the null hypothesis that the distributions  
6 underlying the samples are uncorrelated. The Mann-Whitney-Wilcoxon two-sided test<sup>24</sup> was used for  
7 group-level comparisons with Bonferroni correction<sup>25</sup> for multiple comparisons. The test was performed  
8 using the stat-annot<sup>26</sup> Python library.

9 **Predictive modeling:** Patient-specific loadings were robustly scaled (subtract median, scale by  
10 interquartile range) and used as features in a logistic regression binary classifier. We explored three sets  
11 of features: PSD loadings, PC loadings, and both concatenated together. Nested k-fold cross-validation  
12 (CV) was done to assess variability of model performance on different held-out sets (outer CV loop, 10-  
13 fold) and to tune the ElasticNet regularization strength<sup>41</sup> hyperparameter for each training set (inner CV  
14 loop, 5-fold). Grid for the hyperparameter search ranged between [0, 1] with increments of 0.1. Both CV  
15 loops used disjoint patient splits with target stratification. Loss values were weighted using target class  
16 proportions to handle class imbalance. For each outer CV fold, a classifier was trained using the best  
17 hyperparameter setting found by the inner CV loop and evaluated on the corresponding outer test fold.  
18 We used the area under receiver operating characteristic curve (AUC) to evaluate model performance  
19 across the outer CV folds. Predictive modeling was performed using the scikit-learn<sup>42</sup> Python library.

20 **Data, code, and factor availability:** Summary data and code can be made available by the corresponding  
21 authors upon reasonable request.

22

### 23 3. Results

#### 24 3.1 Characteristics of the Neurological Population, Focal Epilepsy Cohort, and Controls

25 Table 1 provides an overview of the population-level routine EEG dataset. This dataset included 13,652  
26 recordings from 12,134 unique patients. Expert visual review of these EEG recordings based on the Mayo  
27 Clinic grading criteria resulted in 45.7% (N=6,242) normal EEGs, 24.9% (N=3,395) EEGs with mild slowing  
28 (Dysrhythmia grade 1), 13.2% (N=1,800) EEGs with moderate to severe slowing (Dysrhythmia grade 2),  
29 and 16.2% (N=2,215) EEGs with epileptiform abnormalities (Dysrhythmia grade 3). From the population  
30 of Dysrhythmia grade 3 EEGs, we identified 121 focal epilepsy patients with clinically confirmed epilepsy  
31 in either the frontal (N=21) or temporal (N=100) region. In addition, a set of 76 matched non-epileptic  
32 controls with normal EEGs and without a diagnosis of any neurological disease were identified for group  
33 comparisons. Table 2 summarizes the characteristics of the confirmed epilepsy patients and controls.

34

Data Property	Summary Statistics
Routine EEG recordings	Total recordings: 13,652 Unique patients: 12,134



Age	Range: 18-103.7 Mean: 50.9 ( $\pm$ 19.4) Age groups: 18 – 30: 2,639 30 – 50: 3,785 50 – 70: 4,563 >70: 2,665
Sex	Female = 6,464 (53.3%)
EEG Grade (based on expert visual review)	Normal: 6,242 (45.7%) Dysrhythmia 1: 3,395 (24.9%) Dysrhythmia 2: 1,800 (13.2%) Dysrhythmia 3: 2,215 (16.2%)

1

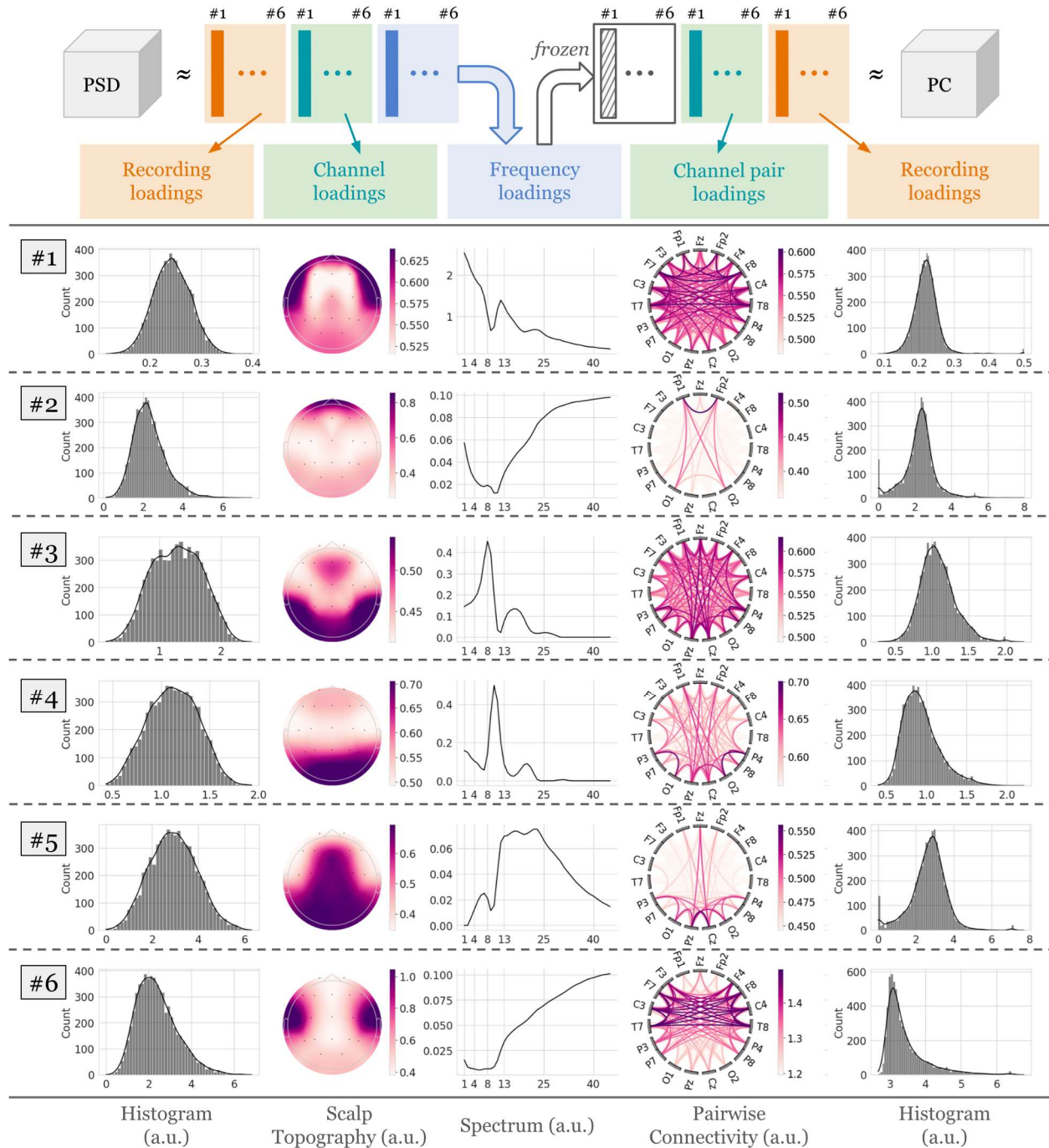
*Table 1: Characteristics of the overall neurologic clinical population.*

Study Cohort	Summary Statistics
Temporal Lobe Epilepsy (TLE)	Unique records: 100 Unique participants: 100 Age: 52.5 (19.9) Sex: 50 (50%) Female Drug response status: 44 Drug-resistant 28 Drug-responsive MRI status: 36 Non-lesional 43 Lesional
Frontal Lobe Epilepsy (FLE)	Unique records: 25 Unique participants: 21 Age: 37.6 (13.6) Sex: 12 (57.1%) Female
Non-epileptic Controls (CTL)	Unique records: 76 Unique participants: 76 Age: 49.2 (19.3) Sex: 41 (53.9%) Female

2

*Table 2: Characteristics of epilepsy cohort and controls used in this study.*

3 **3.2 Tensor Decomposition Extracts Interpretable Spatio-spectral Patterns from Normal EEGs**



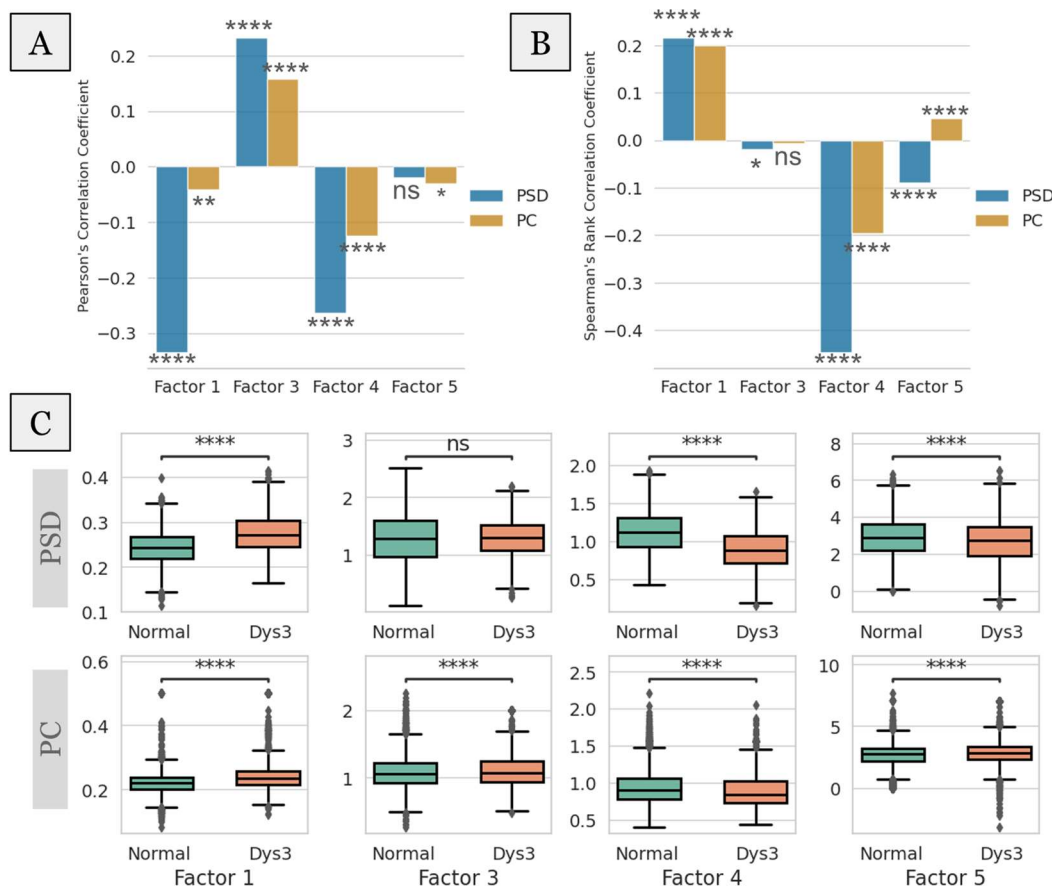
1  
 2 **Figure 2: Data-driven population-level patterns of eyes-closed awake EEG data extracted from 6,242**  
 3 **normal EEGs. Three-dimensional tensors containing spatio-spectral information were decomposed using**  
 4 **non-negative Canonical Polyadic Decomposition to yield six factors. Each row corresponds to a**  
 5 **combination of a power spectral and connectivity-based factors, which is defined by the common**  
 6 **spectral profile, the spatial power distribution over the 19 channels, the pair-wise channel connectivity,**  
 7 **and loadings of EEG recordings in the PSD-tensor and PC-tensor. Recording loadings are visualized as**  
 8 **histograms, spatial activations are visualized as scalp topographical distributions, and spectral**  
 9 **activations are visualized as power spectral density. Note that the PSD-tensor was decomposed first, and**

1 the resulting frequency factors were kept frozen during the decomposition of the PC-tensor to align  
 2 interpretation of the factors. (a.u. refers to absolute units.)

3 Figure 2 shows the factors obtained by decomposing the normal EEGs in the population dataset, i.e., the  
 4 population PSD-tensor and PC-tensor. The frequency profiles are largely distinct, except in the case of  
 5 factors 2 and 6, where their spatial distributions uniquely characterize the overall pattern.

6 Factor 1 shows the characteristic 1/f frequency profile with minor deviations around the oscillatory  
 7 bands and spatial activations in the fronto-temporal and posterior regions, characterizing the  
 8 background non-oscillatory (i.e., aperiodic) brain activity. Factor 2 shows high frequency activations  
 9 (>25Hz) in the prefrontal region, suggesting eye-movement-related artifacts. Factor 3 predominantly  
 10 contains high-theta/low-alpha activity (6-9Hz) in fronto-parietal regions, possibly indicating the high  
 11 theta rhythm or slow alpha rhythm. Factor 4 shows occipital activations in 8-13Hz, resembling the  
 12 characteristic posterior dominant rhythm. Factor 5 shows centro-parietal activations in 13-25Hz,  
 13 capturing the Rolandic beta activity. Lastly, factor 6 shows high-frequency activations (>25Hz) in the  
 14 temporal regions, which may represent muscle artifacts. The analyses and findings presented in the  
 15 remaining text focus on the four putatively physiologic factors (1, 3, 4, and 5).

16 **3.3 Patient Loadings Show Sensitivity to Aging and EEG Dysrhythmia Grades**



17  
 18 **Figure 3: Associations of PSD and PC loadings of the four putatively physiologic factors (1, 3, 4, and 5)**  
 19 **with physiological (aging) and pathological (slowing, epileptiform activity) variables. Factor numbers**  
 20 **correspond to those in Figure 2. Loadings describe activity found in eyes-closed awake EEG segments**

1 selected from expertly graded routine EEGs in the population-level dataset. (A) Correlations of PSD and  
2 PC loadings of normal EEGs with patient age. (B) Correlations of PSD and PC recording loadings with  
3 expert-assigned severity of slowing. The ranked severity levels are 0 (normal EEG, no slowing), 1  
4 (Dysrhythmia 1 EEG, mild slowing), and 2 (Dysrhythmia 2 EEG, moderate to severe slowing) (C)  
5 Correlations of PSD and PC recording loadings with the presence of epileptiform activity (Dysrhythmia 3  
6 EEGs abbreviated as “Dys3”). Significance levels correspond to the Mann-Whitney-Wilcoxon test. Loading  
7 values along y-axes are in arbitrary units. \* indicates a significant correlation with  $p < 0.05$  and \*\*\*\*  
8 indicates a significant correlation with  $p < 1e-4$ .

9

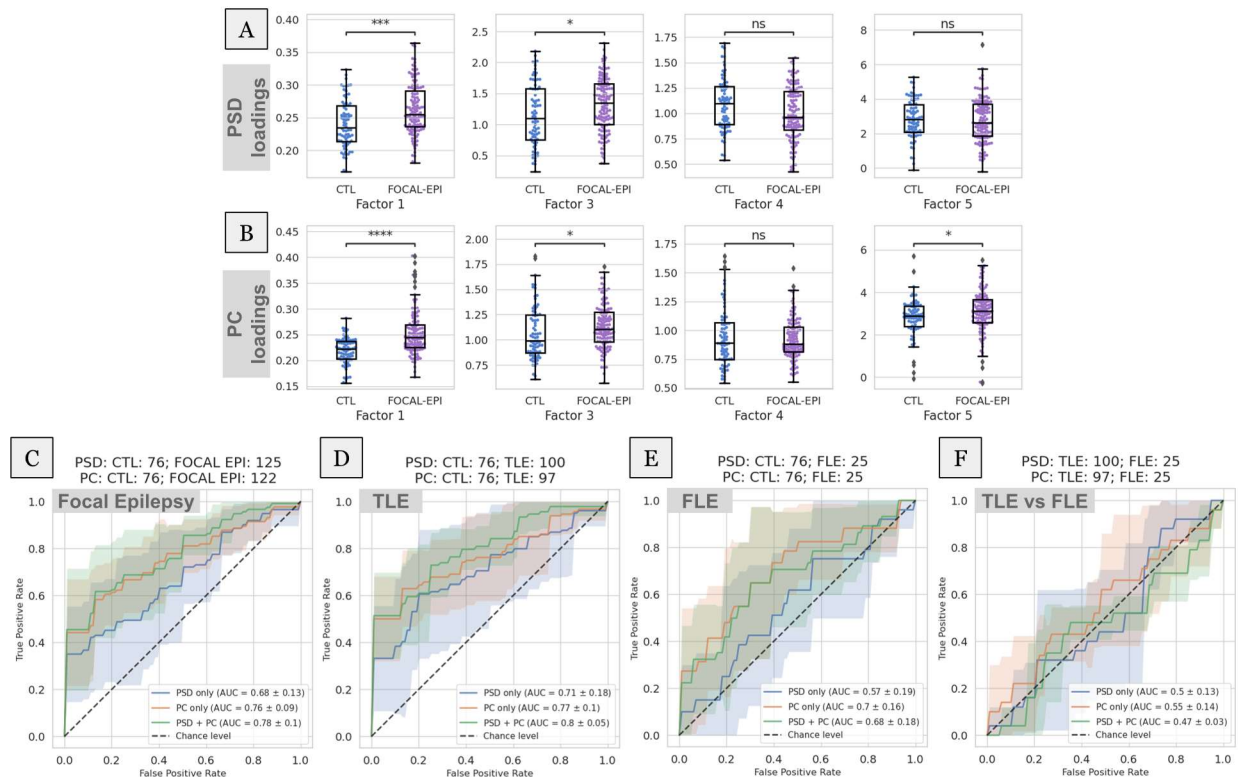
10 Figure 3 shows the associations between the loadings of population EEGs for factors 1, 3, 4, and 5  
11 against patient age and expert-assigned EEG grades

12 *Trends with patient age (Fig. 3A):* Factor 3 is positively correlated with age ( $p < 1e-4$ ), while factors 1 (PSD:  
13  $p < 1e-4$ , PC:  $p < 0.01$ ) and 4 ( $p < 1e-4$ ) are negatively correlated. Although the correlation strength varies  
14 between the PSD and PC loadings of the same factor, they are directionally consistent. Correlations of  
15 factor 5 are either marginally significant (PSD:  $p < 0.05$ ) or not significant (PC).

16 *Trends with expert-ranked degree of slowing (Fig. 3B):* Factor 1 is positively correlated with severity of  
17 slowing ( $p < 1e-4$ ), while factor 4 is negatively correlated ( $p < 1e-4$ ). Correlation of factor 3 is either low  
18 (PSD:  $p < 0.05$ ) or not significant (PC). The correlation of factor 5, although significant ( $p < 1e-4$ ), is  
19 directionally divergent between the PSD and PC loadings.

20 *Differences in presence of epileptiform activity (Fig. 3C):* Here, loadings of EEGs with epileptiform activity  
21 were compared against those of normal EEGs. PSD loadings of factor 1 increase under presence of  
22 epileptiform activity, while those of factors 4 and 5 decrease ( $p < 1e-4$  in every case). Factor 3 PSD  
23 loadings show no significant change. PC loadings of factors 1 and 4 show trends consistent with  
24 corresponding PSD loadings ( $p < 1e-4$  in both cases). However, the PC loadings of factors 3 and 5 show  
25 slight increases ( $p < 1e-4$ ).

26 **3.4 Quantitative Analysis of Normal Interictal EEG Reveals Differences in Focal Epilepsy**



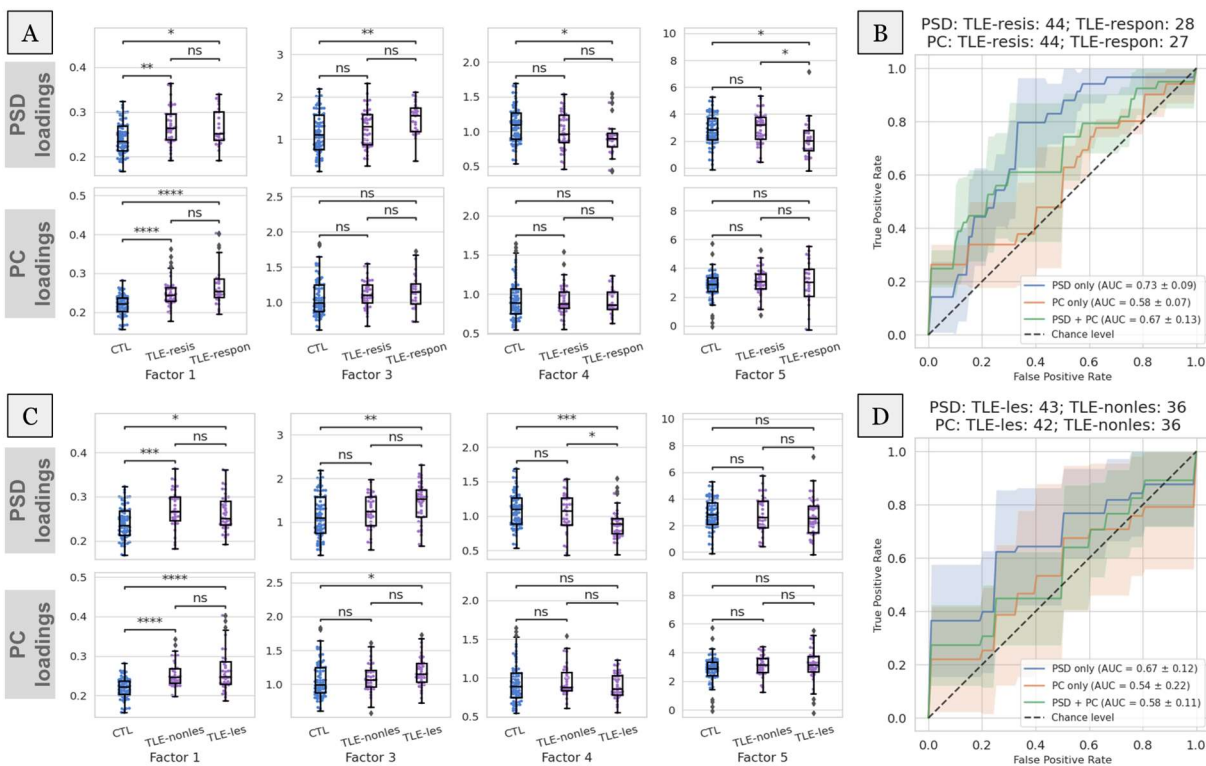
1  
2 **Figure 4: Differentiation of focal epilepsy and epileptogenic.** (A-B) PSD and PC loadings of focal epilepsy  
3 patients (FOCAL-EPI) are compared to those of non-epileptic controls (CTL) across the four physiologic  
4 population factors. Loading values along y-axes are in arbitrary units. \* indicates a significant difference  
5 with  $p < 0.05$  and \*\*\*\* indicates a significant difference with  $p < 1e-4$  in the Mann-Whitney-Wilcoxon  
6 test. (C) PSD and PC loadings are used as features to classify focal epilepsy vs. non-epileptic controls  
7 within a binary classification framework. (D-E) The same classification is broken down by temporal (TLE)  
8 and frontal (FLE) sub-types of focal epilepsy. (F) Differential diagnosis of the epileptogenic lobe, i.e., TLE  
9 vs. FLE, within the focal epilepsy cohort. Note that all classifications used only the four putative  
10 physiologic factors (1, 3, 4, and 5) and were conducted with three sets of features/loadings - only those  
11 of PSD factors ("PSD only"), only those of PC factors ("PC only"), or both concatenated ("PSD + PC").

12 Figure 4 shows results for group differences and binary classifications between non-epileptic controls  
13 and the focal epilepsy cohort using patient-specific PSD and PC loadings of the physiologic factors. We  
14 find focal epilepsy patients to have elevated factor 1 ( $p < 0.001$ ) and factor 3 ( $p < 0.05$ ). In both PSD and PC  
15 comparisons (Figure 4A-B). In addition, we find PC loadings for factor 5 ( $p < 0.05$ ) significantly different in  
16 focal epilepsy relative to non-epileptic controls. Factor 4 loadings do not show significant differences in  
17 either the PSD or PC comparisons.

18 Figure 4C shows classification of focal epilepsy vs. non-epileptic patients is possible above chance levels,  
19 with PC loadings providing the largest contribution to the average classification performance (AUC=0.76).  
20 This performance is marginally improved by using a combination of PSD and PC loadings (AUC=0.78). All  
21 feature sets show high variability in performance across the held-out folds (0.09-0.13). Figures 4D-E  
22 show results for the classification of frontal (FLE) and temporal lobe epilepsy (TLE) against non-epileptic  
23 controls. TLE is better differentiated from non-epileptic patients than FLE (top mean AUC=0.8 vs. 0.7).  
24 TLE is best differentiated by combined PSD and PC loadings (AUC=0.80), with PC loadings contributing

1 the most to classifier performance (AUC=0.77). FLE is best differentiated using PC loadings alone  
 2 (AUC=0.70), and the addition of PSD loadings slightly worsens the performance (AUC=0.68). Variability in  
 3 AUC performance across folds ranges from 0.05-0.19. Lastly, Figure 4F shows the classification of TLE vs  
 4 FLE based on factor loadings derived from normal interictal epochs. Results indicate that none of the  
 5 feature sets can differentiate the epileptogenic lobe (i.e., temporal vs. frontal) in focal epilepsy above  
 6 chance levels (AUCs range between 0.47-0.55) based on normal interictal epochs.

7 **3.5 Quantitative Loadings of Normal Interictal EEG Exhibit Capacity for Differentiation in Drug-**  
 8 **Resistant and Non-lesional Epilepsy**



9  
 10 *Figure 5: Differentiation of drug-resistant and non-lesional temporal lobe epilepsy (TLE) patients using*  
 11 *four physiologic pattern loadings (factors 1, 3, 4, and 5). (A) Loadings are compared between non-*  
 12 *epileptic controls (CTL), TLE patients that are drug resistant (TLE-resis) and those that are drug responsive*  
 13 *(TLE-respon). (B) Binary classifications of drug resistant vs. responsive patients using the same feature*  
 14 *sets as Figure 4. (C-D) Analyses similar to (A) and (B) are conducted for lesional (TLE-les) and non-lesional*  
 15 *(TLE-nonles) TLE sub-groups. Loading values in (A) and (C) along y-axes are in arbitrary units. \* indicates*  
 16 *a significant difference with  $p < 0.05$  and \*\*\*\* indicates a significant difference with  $p < 1e-4$  in the*  
 17 *Mann-Whitney-Wilcoxon test with Bonferroni correction.*

18 Figure 5A shows differences in loadings of non-epileptic controls (CTL), drug-responsive (TLE-respon),  
 19 and drug-resistant (TLE-resis) temporal epilepsy patients. Only the PSD loadings for factor 5 show  
 20 differences between the two sub-groups ( $p < 0.05$ ), while the others show differences only relative to  
 21 controls. None of the PC loadings show significant differences between the two sub-groups. PC loadings  
 22 other than those of factor 1 show no differences between non-epileptic controls and both sub-groups.  
 23 Figure 5B shows the classification performance of different sets of factor loadings in classifying drug

1 resistance. PSD loadings provided the best average performance (AUC=0.73) while PC loadings  
2 performed marginally better than chance (AUC=0.58). Variability in model performance ranged from  
3 0.07 to 0.13 AUC points.

4 Figure 5C shows differences in normal interictal EEG loadings between non-epileptic controls (CTL), non-  
5 lesional (TLE-nonles), and lesional (TLE-les) temporal lobe epilepsy. While PSD loadings of factors 1, 3,  
6 and 4 show significant differences relative to non-epileptic controls for both groups, only factor 4 shows  
7 a significant difference between non-lesional and lesional patients ( $p < 0.05$ ). Trends seen in factors 1 and  
8 3 are similar between the PSD and PC loadings. However, none of the PC loadings differed significantly  
9 between the MRI sub-groups. Figure 5D shows the classification between lesional and non-lesional  
10 patients. PSD loadings best differentiate the two groups of patients with an AUC of 0.67. PC loadings,  
11 either alone or in addition to PSD loadings, significantly worsened the average classification  
12 performance. However, all models exhibited high variability in AUC performance (0.11-0.22 AUC points).

13

#### 14 **4. Discussion**

15 The goal of this study was to explore whether normal interictal EEGs of people with focal epilepsy  
16 contain subtle signals that could be used to augment epilepsy diagnosis and treatment planning,  
17 especially in patients with drug-resistant and MRI normal epilepsy. We proposed a scalable, physiology-  
18 informed, and data-driven tensor decomposition approach that extracts spatio-spectral patterns from a  
19 large population of normal routine EEGs. Each pattern had a distinct signature in the EEG channel  
20 (spatial) and frequency (spectral) dimensions. We obtained patient-specific pattern loadings or  
21 “features” that allowed us to study group differences through statistical comparisons and binary  
22 classifications. Our findings suggest that quantitative description and analysis of visually reviewed  
23 normal routine EEGs has the potential to provide additional value to clinical decision-making in epilepsy.

#### 24 **Tensor Decomposition with Spectral Priors Recovers Interpretable Patterns**

25 This study hypothesized that the information content of normal EEGs can be explained by a  
26 parsimonious number of latent patterns. To test this hypothesis, we decomposed the spectral and  
27 connectivity contents of a population of normal routine EEGs into several meaningful patterns (i.e.,  
28 factors) using a canonical polyadic tensor decomposition. In general, determining the exact number of  
29 factors, i.e., the presumed rank of the population tensor, is challenging and involves trial-and-error<sup>43</sup>.  
30 However, prior work has demonstrated that the morphological content of the scalp EEG PSD can be  
31 sufficiently explained by six physiological components, namely one aperiodic 1/f pattern and five  
32 oscillatory bands<sup>35</sup>. We used this spectral parameterization model to construct six corresponding  
33 frequency priors that, in turn, provided the spectral initialization as well as an appropriate rank for the  
34 decomposition. Furthermore, we fixed the spectral patterns extracted from PSD-tensor during the  
35 decomposition of PC-tensor to recover semantically consistent patterns from both the tensor types.

36 Several prior works have explored data-driven or unsupervised recovery of spatial, spectral, or temporal  
37 profiles of oscillatory sources and background patterns comprising spontaneous EEG activity<sup>44-48</sup>. In this  
38 study, we presented an approach that quantifies spatio-spectral EEG patterns with the goal of decision  
39 support when clinical EEGs are normal on expert visual review. Beyond the use of spectral-prior-based

1 initialization, our approach did not place any assumptions on the statistical nature or morphology of the  
2 latent EEG patterns and can be applied without sophisticated artifact removal.

3 The population patterns (Fig. 2) can be loosely interpreted to reflect dominant and overlapping  
4 physiological processes whose linear superposition (summation) yields the original EEG trace. We then  
5 interpreted the identified patterns based on clinical domain knowledge. The putative interpretations of  
6 these patterns are supported by their sensitivity to patient age and severity of pathology (Fig. 3).

## 7 **Augmenting Epilepsy Diagnosis and Treatment Planning**

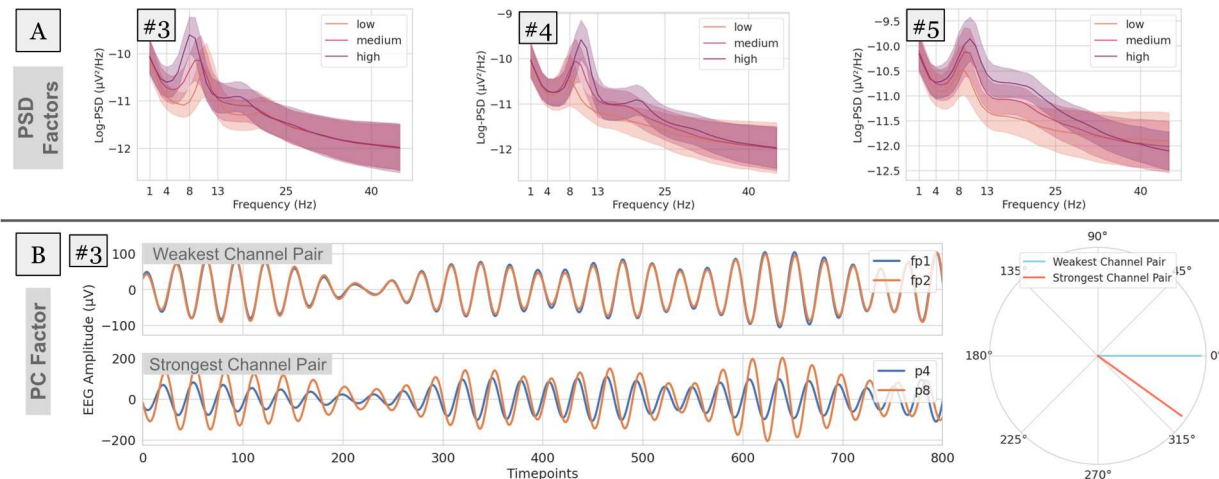
8 Scalp EEG is an indispensable tool in epilepsy that can non-invasively record brain electrical activity with  
9 excellent temporal resolution. Due to this unique resolution, scalp EEG tests can capture transient  
10 interictal epileptiform discharges (IEDs) such as epileptiform spikes or sharp waves associated with  
11 epilepsy<sup>49</sup>. In current clinical practice, the expert identification and characterization of IEDs on routine  
12 scalp EEG is crucial for epilepsy diagnosis. Routine EEGs are also useful in measuring the efficacy of  
13 ongoing ASM trials<sup>50</sup>. In the case of drug-resistant epilepsy, the distribution of IEDs identified on scalp  
14 EEGs can help localize the seizure onset zone, especially in patients with no visible lesion on MRI. Thus,  
15 the identification of IEDs is central to the clinical value of scalp EEGs in current practice.

16 Recent studies have shown significant interest in the automated identification of IEDs to augment expert  
17 visual review<sup>51–53</sup>. However, the diagnostic yield of a single routine scalp EEG is limited, with only 29-55%  
18 of them capturing epileptiform abnormalities<sup>54</sup>. Multiple EEGs may increase epileptiform yield up to  
19 ~75%<sup>55,56</sup>, but the expected gain sharply drops after the third normal EEG. As such, normal interictal EEGs  
20 can cause treatment delays in multiple stages of epilepsy care. Previous studies that explored biomarkers  
21 of interictal non-epileptiform EEG support the possibility of augmenting decision support in epilepsy  
22 using spectral and connectivity-based EEG features<sup>17–19,23,57–61</sup>. Drawing inspiration from these smaller  
23 scale studies, we explored data-driven recovery of spectral features using a large population dataset of  
24 normal EEGs and analyzed their differences in epilepsy.

25 Our findings in Figures 4 and 5 suggest that normal interictal EEG activity of focal epilepsy patients  
26 contains significant differences in putative physiologic oscillations (factors 3, 4, and 5) as well as  
27 aperiodic 1/f(Hz) activity (factor 1). Increases in expression of 1/f and theta frequency activity, coupled  
28 with a decrease in alpha frequency may represent general intermittent slowing of the EEG background.  
29 Although we identified differences in factor 5, the differences in beta frequency rhythm may arise due to  
30 the presence of ASMs. The factors exhibited relatively lower performance in detecting FLE (Fig. 4E) and  
31 in differentiating FLE vs TLE (Fig. 4F). We believe that this may be due to either the lower sample size of  
32 the FLE cohort compared to the TLE cohort (Fig. 4D) or the global/symmetric nature of the population  
33 patterns.

## 34 **Understanding Subtle Variation in Visibly Normal EEGs through their Quantitative Descriptors**





1  
2 *Figure 6: Variability in EEG power and phase characteristics based on factor loading values. (A) Variability*  
3 *in the power spectra of EEGs whose PSD loadings score in the bottom 10-percentile (low), between 40-*  
4 *60-percentile (medium), and top 10-percentile (high). Examples are shown for factors 3, 4, and 5. (B) 8-*  
5 *Hz-filtered EEG traces of the weakest (top) and strongest (bottom) channel pairs for an example EEG that*  
6 *scored in the top 10-percentile for factor 3 (whose spectral power peaks at 8Hz). Overlapping EEG traces*  
7 *reveal phase relationships, i.e., time lags that maximize correlation within the channel pairs. These lags*  
8 *or phase differences are visualized in polar coordinates (right).*

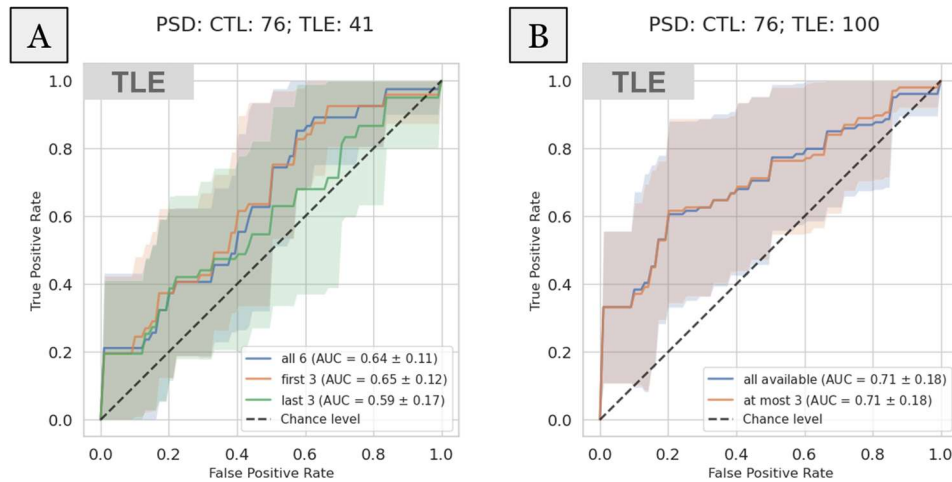
9 Our results (Figure 4) indicate that factor loadings extracted from normal EEG segments have the  
10 potential to classify focal epilepsy above chance levels (best mean AUC=0.78). We analyzed the changes  
11 in actual power spectral and timeseries data corresponding to the changes in factor loadings to further  
12 illuminate the factor interpretations.

13 Fig. 6A shows the full power spectra of normal EEG segments whose loadings fall in the bottom 10-  
14 percentile (low), between 40-60-percentile (medium) and top 10-percentile (high) of a particular  
15 physiologic oscillatory factor. We find that EEGs that score high in factors 3, 4, and 5 have higher power  
16 in high-theta/low-alpha, alpha, and beta bands, respectively.

17 Effects of the phase-lag-based connectivity (i.e., wPLI) at a particular frequency can be observed by  
18 leading/lagging relationships in the time-domain EEG signal filtered at that frequency. Fig. 6B focuses on  
19 factor 3 whose spectral power peaks at 8Hz, with the weakest edge connecting Fp1 and Fp2, and the  
20 strongest edge connecting P4 and P8 (shown in Figure 2). We visualize the phase relationships using an  
21 example EEG segment whose loading value was in the top 10-percentile for factor 3 after filtering its EEG  
22 trace around 8-Hz to. We find that the strongest channel pair (Fig 6B, bottom) has a consistent non-zero  
23 phase difference, while the weakest channel pair (Fig 6B, top) has no phase difference. These phase  
24 differences can be quantified by the time lag that maximizes timeseries correlation within the channel  
25 pair and are visualized in polar coordinates (Fig 6B, right).

26 These illustrations highlight that the quantitative loading values provided by this tensor-based  
27 framework are interpretable based on physiologically relevant concepts such as signal power and phase  
28 and offer sensitivity to subtle changes in the EEG signal. These subtle changes in normal EEGs are likely  
29 to be missed during traditional expert visual review, which focuses mostly on transient abnormalities in  
30 the time domain.

## 1 Influence of Sample Size and Selected EEG Epochs on Study Findings



2  
3 *Figure 7: Repeated CTL vs TLE classifications using two bootstraps to evaluate bias introduced by the*  
4 *dataset selection process. Strategy A (left) uses either the first or last three of the six EEG epochs from a*  
5 *subset of TLE patients (N=41). Strategy B (right) uses at most 3 epochs that are randomly chosen but uses*  
6 *all available TLE patients (N=100).*

7 The routine EEG protocol contained diverse patient states (eyes-closed, eyes-open, awake, drowsy,  
8 asleep) and provocative maneuvers<sup>62</sup> (photic stimulation, hyperventilation, sleep deprivation), making it  
9 necessary to select EEG epochs corresponding to a fixed patient state for data analysis. Such data  
10 selection may introduce bias in our findings since we selected only a maximum of six EEG epochs from  
11 each recording for our analyses.

12 To evaluate whether a bias exists, we repeated the controls vs TLE classification (result in Fig. 4D) with  
13 two bootstrapping strategies, whose results are shown in Figure 7. In strategy A (Fig. 7A), we considered  
14 TLE patients (N=41) with exactly six normal interictal EEG epochs and showed differences in classification  
15 performance depending on which 50% data are used for classification (i.e., first three epochs or last  
16 three epochs). Mean performance was higher when the first 3 epochs were used (AUC=0.65) than last 3  
17 epochs (AUC=0.59). In strategy B (Fig. 7B), we maintained the sample size of the original TLE cohort  
18 (N=100) but used at most three randomly picked EEG epochs per recording to perform classification. For  
19 patients with >3 epochs available, 3 epochs were randomly chosen and for those patients with ≤3  
20 epochs, all epochs were chosen. Our results did not show any significant differences between those two  
21 sampling approaches and the overall performance closely matched that using all available epochs.

22 These results suggest that: 1) our findings may be sensitive to low cohort size but are less likely to be  
23 biased by the algorithmic selection of EEG epochs within a recording, and 2) even as few as three normal  
24 interictal EEG epochs (30 seconds) are sufficient to derive a pretest measure of TLE.

## 25 Study Limitations

26 Our goal in this study was to evaluate whether a quantitative analysis of normal EEG segments of  
27 epilepsy patients can indicate the possible presence of focal epilepsy. To test this hypothesis, we  
28 analyzed non-epileptiform interictal segments identified by a board-certified epileptologist within EEG  
29 recordings containing epileptiform abnormalities at other times (i.e., Dysrhythmia grade 3). However, an

1 analysis using entirely normal EEGs of epilepsy patients will be necessary to evaluate the true potential  
2 of our results. However, identification of such EEGs requires extensive review of patient records, which  
3 we hope to accomplish in a follow-up study. Furthermore, eyes-closed wakefulness was determined by a  
4 heuristic algorithm validated in previous studies<sup>23,63</sup>. Events markers or comments added by EEG  
5 technologists<sup>70</sup> during the EEG study could help to identify the patient's behavioral state more reliably.  
6 Extension of our analysis to different sleep states will be pursued in future studies.

7 The estimation of connectivity could benefit from EEG source modeling to avoid volume conduction<sup>71</sup>  
8 and active reference<sup>72</sup> effects on the scalp. However, the lower spatial density of clinical EEGs prevented  
9 source/inverse modeling efforts, as previous studies have shown that EEG source modeling with fewer  
10 than 64 channels is highly error-prone<sup>65-67</sup>. Phase-based connectivity, and wPLI in particular, was chosen  
11 to suppress spurious zero-lag correlations and partially alleviate the effects of volume conduction<sup>67,68</sup>.  
12 Due to absence of patient-specific head models, average referencing was chosen to mitigate reference-  
13 related effects on connectivity better than alternatives like Cz and linked mastoids<sup>69</sup>.

14 Our classification analyses demonstrated a high level of variance between cross-validation folds (Fig. 4  
15 and Fig. 5). Such variance could be a result of low sample size and the potential effects of  
16 comorbidities<sup>70,71</sup> and medications<sup>72</sup>. The effects of these confounders may be mitigated either by  
17 comprehensive patient review to identify a clinically homogeneous set of focal epilepsy patients or with  
18 the use of larger epilepsy and matched control cohorts. Given that the EEG background patterns  
19 identified in this study are not specific to epilepsy, apparent differences in factor loadings must be  
20 interpreted within the appropriate clinical context. Additionally, validations using normal interictal EEGs  
21 from an external site are needed to assess the generalizability of the presented findings.

22

## 23 **5. Conclusion**

24 Normal interictal EEGs recorded from epilepsy patients can lead to delays in neurological care, especially  
25 in patients with drug-resistant and normal MRI epilepsy. This study explored the value of quantitative  
26 analysis of normal interictal EEGs in supporting a focal epilepsy diagnosis. Application of this  
27 unsupervised learning approach could benefit treatment planning in the future. We presented a  
28 scalable, interpretable, data-driven approach based on canonical polyadic decomposition that recovered  
29 physiologically meaningful spectral power and phase-based connectivity patterns from a population-  
30 scale dataset of normal EEGs and provided patient-specific loadings for each pattern. These loadings  
31 demonstrated value in classifying focal epilepsy and, in temporal lobe epilepsy, drug resistance and  
32 absence of lesions. These findings suggest that normal routine EEGs may contain subtle abnormalities  
33 that can be captured using a quantitative approach and be potentially used to augment decision-making  
34 in clinically challenging scenarios.

35

## 36 **Acknowledgements**

37 We thank the Mayo Clinic Neurology Artificial Intelligence Program (NAIP) for guidance on the data  
38 processing workflow.

39

1    **Funding**

2    This study was supported in part by a Mayo Clinic Illinois Alliance Fellowship for Technology-based  
3    Healthcare Research, NSF grants IIS-2105233, IIS-2344731, and IIS-2337909, and NIH grants R01-  
4    NS092882 and UG3 NS123066.

5

6    **Competing Interests**

7    None

8

## 1   **References**

- 2   1. Epilepsy: a public health imperative. [https://www.who.int/publications/i/item/epilepsy-a-public-](https://www.who.int/publications/i/item/epilepsy-a-public-health-imperative)  
3    health-imperative.
- 4   2. Noachtar, S. & Rémi, J. The role of EEG in epilepsy: A critical review. *Epilepsy Behav.* **15**, 22–33  
5    (2009).
- 6   3. Smith, S. EEG in the diagnosis, classification, and management of patients with epilepsy. *J.*  
7    *Neurol. Neurosurg. Psychiatry* **76**, ii2–ii7 (2005).
- 8   4. Worrell, G. A., Lagerlund, T. D. & Buchhalter, J. R. Role and Limitations of Routine and  
9    Ambulatory Scalp Electroencephalography in Diagnosing and Managing Seizures. *Mayo Clin.*  
10   *Proc.* **77**, 991–998 (2002).
- 11   5. Holmes, G. L. Interictal Spikes as an EEG Biomarker of Cognitive Impairment. *J. Clin.*  
12    *Neurophysiol. Off. Publ. Am. Electroencephalogr. Soc.* **39**, 101–112 (2022).
- 13   6. Hughes, J. R. The Significance of the Interictal Spike Discharge: A Review. *J. Clin. Neurophysiol.*  
14    **6**, 207 (1989).
- 15   7. Benbadis, S. R., Beniczky, S., Bertram, E., MacIver, S. & Moshé, S. L. The role of EEG in patients  
16    with suspected epilepsy. *Epileptic. Disord.* **22**, 143–155 (2020).
- 17   8. Baldin, E., Hauser, W. A., Buchhalter, J. R., Hesdorffer, D. C. & Ottman, R. Yield of epileptiform  
18    electroencephalogram abnormalities in incident unprovoked seizures: A population-based  
19    study. *Epilepsia* **55**, 1389–1398 (2014).
- 20   9. Schreiner, A. & Pohlmann-Eden, B. Value of the Early Electroencephalogram after a First  
21    Unprovoked Seizure. *Clin. Electroencephalogr.* **34**, 140–144 (2003).
- 22   10.    Burkholder, D. B. *et al.* Routine vs extended outpatient EEG for the detection of interictal  
23    epileptiform discharges. *Neurology* **86**, 1524–1530 (2016).

- 1 11. Narayanan, J. T., Labar, D. R. & Schaul, N. Latency to first spike in the EEG of epilepsy  
2 patients. *Seizure - Eur. J. Epilepsy* **17**, 34–41 (2008).
- 3 12. Marsan, C. A. & Zivin, L. S. Factors Related to the Occurrence of Typical Paroxysmal  
4 Abnormalities in the EEG Records of Epileptic Patients. *Epilepsia* **11**, 361–381 (1970).
- 5 13. Pillai, J. & Sperling, M. R. Interictal EEG and the Diagnosis of Epilepsy. *Epilepsia* **47**, 14–22  
6 (2006).
- 7 14. Chen, Z., Brodie, M. J., Liew, D. & Kwan, P. Treatment Outcomes in Patients With Newly  
8 Diagnosed Epilepsy Treated With Established and New Antiepileptic Drugs: A 30-Year  
9 Longitudinal Cohort Study. *JAMA Neurol.* **75**, 279–286 (2018).
- 10 15. Kwan, P. & Brodie, M. J. Early identification of refractory epilepsy. *N. Engl. J. Med.* **342**, 314–  
11 319 (2000).
- 12 16. Cendes, F., Theodore, W. H., Brinkmann, B. H., Sulc, V. & Cascino, G. D. Chapter 51 -  
13 Neuroimaging of epilepsy. in *Handbook of Clinical Neurology* (eds. Masdeu, J. C. & González, R.  
14 G.) vol. 136 985–1014 (Elsevier, 2016).
- 15 17. Wagh, N. & Varatharajah, Y. EEG-GCNN: Augmenting Electroencephalogram-based  
16 Neurological Disease Diagnosis using a Domain-guided Graph Convolutional Neural Network. in  
17 *Proceedings of the Machine Learning for Health NeurIPS Workshop* 367–378 (PMLR, 2020).
- 18 18. Varatharajah, Y. *et al.* Electrophysiological Correlates of Brain Health Help Diagnose  
19 Epilepsy and Lateralize Seizure Focus. in *2020 42nd Annual International Conference of the IEEE*  
20 *Engineering in Medicine & Biology Society (EMBC)* 3460–3464 (2020).  
21 doi:10.1109/EMBC44109.2020.9176668.
- 22 19. Varatharajah, Y. *et al.* Characterizing the electrophysiological abnormalities in visually  
23 reviewed normal EEGs of drug-resistant focal epilepsy patients. *Brain Commun.* **3**, fcab102  
24 (2021).

- 1 20. Varatharajah, Y. *et al.* Quantitative analysis of visually reviewed normal scalp EEG predicts  
2 seizure freedom following anterior temporal lobectomy. *Epilepsia* **63**, 1630–1642 (2022).
- 3 21. Li, W. *et al.* Data-driven retrieval of population-level EEG features and their role in  
4 neurodegenerative diseases. *Brain Commun.* **6**, fcae227 (2024).
- 5 22. Report of the committee on methods of clinical examination in electroencephalography:  
6 1957. *Electroencephalogr. Clin. Neurophysiol.* **10**, 370–375 (1958).
- 7 23. Varatharajah, Y. *et al.* Quantitative analysis of visually reviewed normal scalp EEG predicts  
8 seizure freedom following anterior temporal lobectomy. *Epilepsia* **63**, 1630–1642 (2022).
- 9 24. Vallat, R. & Walker, M. P. An open-source, high-performance tool for automated sleep  
10 staging. *eLife* **10**, e70092 (2021).
- 11 25. Harris, C. R. *et al.* Array programming with NumPy. *Nature* **585**, 357–362 (2020).
- 12 26. Gramfort, A. *et al.* MEG and EEG data analysis with MNE-Python. *Front. Neurosci.* **7**, (2013).
- 13 27. Schiratti, J.-B., Le Douget, J.-E., Le Van Quyen, M., Essid, S. & Gramfort, A. An Ensemble  
14 Learning Approach to Detect Epileptic Seizures from Long Intracranial EEG Recordings. in *2018*  
15 *IEEE International Conference on Acoustics, Speech and Signal Processing (ICASSP)* 856–860  
16 (2018). doi:10.1109/ICASSP.2018.8461489.
- 17 28. Vallat, R. & Walker, M. P. An open-source, high-performance tool for automated sleep  
18 staging. *eLife* **10**, e70092 (2021).
- 19 29. Welch, P. The use of fast Fourier transform for the estimation of power spectra: A method  
20 based on time averaging over short, modified periodograms. *IEEE Trans. Audio Electroacoustics*  
21 **15**, 70–73 (1967).
- 22 30. Vinck, M., Oostenveld, R., van Wingerden, M., Battaglia, F. & Pennartz, C. M. A. An improved  
23 index of phase-synchronization for electrophysiological data in the presence of volume-  
24 conduction, noise and sample-size bias. *NeuroImage* **55**, 1548–1565 (2011).

- 1 31. Hitchcock, F. L. Multiple Invariants and Generalized Rank of a P-Way Matrix or Tensor. *J.*  
2 *Math. Phys.* **7**, 39–79 (1928).
- 3 32. Hitchcock, F. L. The Expression of a Tensor or a Polyadic as a Sum of Products. *J. Math.*  
4 *Phys.* **6**, 164–189 (1927).
- 5 33. Harshman, R. A. FOUNDATIONS OF THE PARAFAC PROCEDURE: MODELS AND  
6 CONDITIONS FOR AN ‘EXPLANATORY’ MULTIMODAL FACTOR ANALYSIS.
- 7 34. Carroll, J. D. & Chang, J.-J. Analysis of individual differences in multidimensional scaling via  
8 an n-way generalization of “Eckart-Young” decomposition. *Psychometrika* **35**, 283–319 (1970).
- 9 35. Donoghue, T. *et al.* Parameterizing neural power spectra into periodic and aperiodic  
10 components. *Nat. Neurosci.* **23**, 1655–1665 (2020).
- 11 36. Williams, A. H. *et al.* Unsupervised Discovery of Demixed, Low-Dimensional Neural  
12 Dynamics across Multiple Timescales through Tensor Component Analysis. *Neuron* **98**, 1099-  
13 1115.e8 (2018).
- 14 37. Gupta, T. *et al.* Tensor Decomposition of Large-scale Clinical EEGs Reveals Interpretable  
15 Patterns of Brain Physiology. in *2023 11th International IEEE/EMBS Conference on Neural*  
16 *Engineering (NER)* 1–4 (2023). doi:10.1109/NER52421.2023.10123800.
- 17 38. Mann, H. B. & Whitney, D. R. On a Test of Whether one of Two Random Variables is  
18 Stochastically Larger than the Other. *Ann. Math. Stat.* **18**, 50–60 (1947).
- 19 39. Bland, J. M. & Altman, D. G. Multiple significance tests: the Bonferroni method. *BMJ* **310**,  
20 170 (1995).
- 21 40. Charlier, F. *et al.* trevismd/statannotations: v0.6. Zenodo  
22 <https://doi.org/10.5281/zenodo.8396665> (2023).
- 23 41. Zou, H. & Hastie, T. Regularization and Variable Selection Via the Elastic Net. *J. R. Stat. Soc.*  
24 *Ser. B Stat. Methodol.* **67**, 301–320 (2005).



- 1 42. Pedregosa, F. *et al.* Scikit-learn: Machine Learning in Python. *J. Mach. Learn. Res.* **12**, 2825–  
2 2830 (2011).
- 3 43. Tensor Decomposition for Signal Processing and Machine Learning.  
4 <https://ieeexplore.ieee.org/abstract/document/7891546>.
- 5 44. Koles, Z. J. The quantitative extraction and topographic mapping of the abnormal  
6 components in the clinical EEG. *Electroencephalogr. Clin. Neurophysiol.* **79**, 440–447 (1991).
- 7 45. Nikulin, V. V., Nolte, G. & Curio, G. A novel method for reliable and fast extraction of  
8 neuronal EEG/MEG oscillations on the basis of spatio-spectral decomposition. *NeuroImage* **55**,  
9 1528–1535 (2011).
- 10 46. Hyvärinen, A., Ramkumar, P., Parkkonen, L. & Hari, R. Independent component analysis of  
11 short-time Fourier transforms for spontaneous EEG/MEG analysis. *NeuroImage* **49**, 257–271  
12 (2010).
- 13 47. Miwakeichi, F. *et al.* Decomposing EEG data into space–time–frequency components using  
14 Parallel Factor Analysis. *NeuroImage* **22**, 1035–1045 (2004).
- 15 48. Bridwell, D. A., Rachakonda, S., Rogers, F. S., Pearlson, G. D. & Calhoun, V. D.  
16 Spatospectral decomposition of multi-subject EEG: evaluating blind source separation  
17 algorithms on real and realistic simulated data. *Brain Topogr.* **31**, 47–61 (2018).
- 18 49. Sundaram, M., Hogan, T., Hiscock, M. & Pillay, N. Factors affecting interictal spike  
19 discharges in adults with epilepsy. *Electroencephalogr. Clin. Neurophysiol.* **75**, 358–360 (1990).
- 20 50. Höller, Y., Helmstaedter, C. & Lehnertz, K. Quantitative Pharmaco-Electroencephalography  
21 in Antiepileptic Drug Research. *CNS Drugs* **32**, 839–848 (2018).
- 22 51. Tveit, J. *et al.* Automated Interpretation of Clinical Electroencephalograms Using Artificial  
23 Intelligence. *JAMA Neurol.* **80**, 805–812 (2023).

- 1 52. Gemein, L. A. W. *et al.* Machine-learning-based diagnostics of EEG pathology. *NeuroImage*  
2 **220**, 117021 (2020).
- 3 53. Beniczky, S. *et al.* Standardized Computer-based Organized Reporting of EEG: SCORE.  
4 *Epilepsia* **54**, 1112–1124 (2013).
- 5 54. Burkholder, D. B. *et al.* Routine vs extended outpatient EEG for the detection of interictal  
6 epileptiform discharges. *Neurology* **86**, 1524–1530 (2016).
- 7 55. Doppelbauer, A. *et al.* Occurrence of epileptiform activity in the routine EEG of epileptic  
8 patients. *Acta Neurol. Scand.* **87**, 345–352 (1993).
- 9 56. Baldin, E., Hauser, W. A., Buchhalter, J. R., Hesdorffer, D. C. & Ottman, R. Yield of  
10 epileptiform EEG abnormalities in incident unprovoked seizures: a population-based study.  
11 *Epilepsia* **55**, 1389–1398 (2014).
- 12 57. Pyrzowski, J., Siemiński, M., Sarnowska, A., Jedrzejczak, J. & Nyka, W. M. Interval analysis of  
13 interictal EEG: pathology of the alpha rhythm in focal epilepsy. *Sci. Rep.* **5**, 16230 (2015).
- 14 58. Larsson, P. G. & Kostov, H. Lower frequency variability in the alpha activity in EEG among  
15 patients with epilepsy. *Clin. Neurophysiol.* **116**, 2701–2706 (2005).
- 16 59. Woldman, W. *et al.* Dynamic network properties of the interictal brain determine whether  
17 seizures appear focal or generalised. *Sci. Rep.* **10**, 7043 (2020).
- 18 60. Pegg, E. J., Taylor, J. R., Laiou, P., Richardson, M. & Mohanraj, R. Interictal  
19 electroencephalographic functional network topology in drug-resistant and well-controlled  
20 idiopathic generalized epilepsy. *Epilepsia* **62**, 492–503 (2021).
- 21 61. Verhoeven, T. *et al.* Automated diagnosis of temporal lobe epilepsy in the absence of  
22 interictal spikes. *NeuroImage Clin.* **17**, 10–15 (2018).
- 23 62. Beniczky, S. & Schomer, D. L. Electroencephalography: basic biophysical and technological  
24 aspects important for clinical applications. *Epileptic. Disord.* **22**, 697–715 (2020).

- 1 63. Li, W. *et al.* Data-driven retrieval of population-level EEG features and their role in  
2 neurodegenerative diseases. *Brain Commun.* **6**, fcae227 (2024).
- 3 64. Saab, K., Dunnmon, J., Ré, C., Rubin, D. & Lee-Messer, C. Weak supervision as an efficient  
4 approach for automated seizure detection in electroencephalography. *Npj Digit. Med.* **3**, 1–12  
5 (2020).
- 6 65. Akalin Acar, Z. & Makeig, S. Effects of Forward Model Errors on EEG Source Localization.  
7 *Brain Topogr.* **26**, 378–396 (2013).
- 8 66. Lantz, G., Grave de Peralta, R., Spinelli, L., Seeck, M. & Michel, C. M. Epileptic source  
9 localization with high density EEG: how many electrodes are needed? *Clin. Neurophysiol.* **114**,  
10 63–69 (2003).
- 11 67. Brodbeck, V. *et al.* Electroencephalographic source imaging: a prospective study of 152  
12 operated epileptic patients. *Brain* **134**, 2887–2897 (2011).
- 13 68. Stam, C. J., Nolte, G. & Daffertshofer, A. Phase lag index: Assessment of functional  
14 connectivity from multi channel EEG and MEG with diminished bias from common sources.  
15 *Hum. Brain Mapp.* **28**, 1178–1193 (2007).
- 16 69. Vinck, M., Oostenveld, R., van Wingerden, M., Battaglia, F. & Pennartz, C. M. A. An improved  
17 index of phase-synchronization for electrophysiological data in the presence of volume-  
18 conduction, noise and sample-size bias. *NeuroImage* **55**, 1548–1565 (2011).
- 19 70. Chella, F., Pizzella, V., Zappasodi, F. & Marzetti, L. Impact of the reference choice on scalp  
20 EEG connectivity estimation. *J. Neural Eng.* **13**, 036016 (2016).
- 21 71. Keezer, M. R., Sisodiya, S. M. & Sander, J. W. Comorbidities of epilepsy: current concepts  
22 and future perspectives. *Lancet Neurol.* **15**, 106–115 (2016).
- 23 72. Hesdorffer, D. C. Comorbidity between neurological illness and psychiatric disorders. *CNS*  
24 *Spectr.* **21**, 230–238 (2016).

- 1 73. Recognizing Artifacts and Medication Effects. in *Critical Care EEG Basics: Rapid Bedside*
- 2 *EEG Reading for Acute Care Providers* (eds. Rossi, K. C. & Jadeja, N. M.) 41–70 (Cambridge
- 3 University Press, Cambridge, 2024). doi:10.1017/9781009261159.007.
- 4